RESEARCH ARTICLE

Lycium barbarum polysaccharides related RAGE and Aβ levels in the retina of mice with acute ocular hypertension and promote maintenance of blood retinal barrier

Xue-Song Mi[1, 3], **Qian Feng**[2, 4, 7], **Amy Cheuk Yin Lo**[5], **Raymond Chuen-Chung Chang**[4, 7], **Sookja Kim Chung**[6, 7], **Kwok-Fai So**[2, 3, 4, 5, *]

1 Department of Ophthalmology, the First Affiliated Hospital of Jinan University, Guangzhou, Guangdong Province, China
2 Guangdong-Hong Kong-Macau Institute of CNS Regeneration, Jinan University, Guangzhou, Guangdong Province, China
3 Changsha Academician Expert Workstation, Aier Eye Hospital Group, Changsha, Hunan Province, China
4 State Key Laboratory of Brain and Cognitive Sciences, Hong Kong Special Administrative Region, China
5 Department of Ophthalmology, The University of Hong Kong, Hong Kong Special Administrative Region, China
6 Faculty of Medicine, Macau University of Science and Technology, Macao Special Administrative Region, China
7 School of Biomedical Science, LKS Faculty of Medicine, The University of Hong Kong, Hong Kong Special Administrative Region, China

Funding: *This study was supported in part by the National Basic Research Program of China, No. 81300766 (to XSM); the Cultivation and Innovation Fund from the First Affiliated Hospital of Jinan University, China, No. 802168 (to XSM); Hygiene & Health Appropriated Technology and Promoting Project of Guangdong Province of China, No. 201905270933056876 (to XSM); the fund of Leading Talents of Guangdong Province of China, No. 87014002 (to KFS); a grant from Ningxia Key Research and Development Program, and Programme of Introducing Talents of Discipline to Universities of China, No. B14036 (to KFS).*

Graphical Abstract

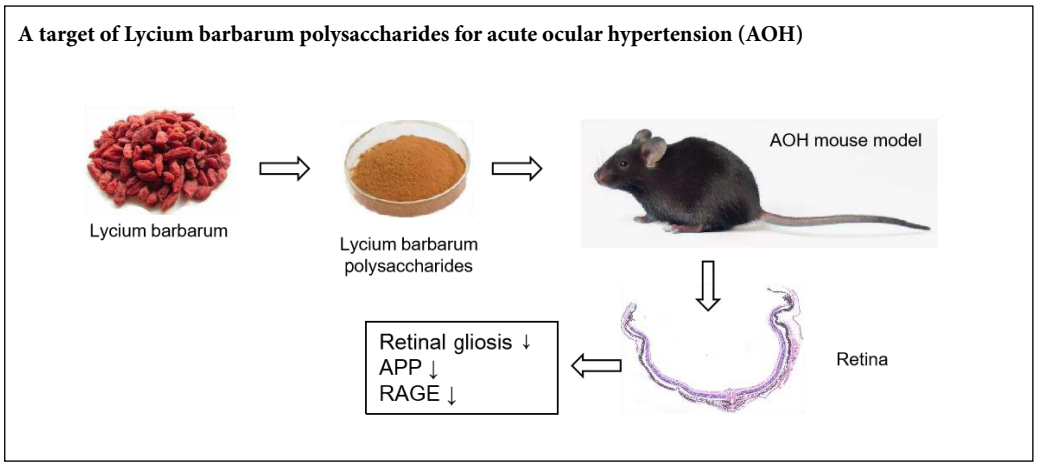

Correspondence to:
Kwok-Fai So, PhD, hrmaskf@hku.hk.

orcid:
0000-0003-4039-4246
(Kwok-Fai So)

doi: *10.4103/1673-5374.284998*

Received: *February 17, 2020*
Peer review started: *February 28, 2020*
Accepted: *April 1, 2020*
Published online: *June 19, 2020*

Abstract

Our previous study verified the protective effects of Lycium barbarum polysaccharides (LBP) on retinal neurons and blood vessels in acute ocular hypertension (AOH) mice. To investigate the effect of LBP on the reactivity of retinal glial cells, an AOH mouse model was established in one eye by maintaining ocular hypertension of 90 mmHg for 60 minutes. Either LBP solution (1 mg/kg) or phosphate-buffered saline was administrated to the mice by gavage daily, starting 7 days before the AOH insult and continuing until the mice were sacrificed for specimen collection on day 4 post-insult. After AOH insult, increased numbers of astrocytes and microglia were observed, together with decreased expression of the following glial cell biomarkers in the retinal ganglion cells of AOH mice: glial fibrillary acidic protein, glutamine synthetase, aquaporin-4, S-100 proteins, ionized calcium-binding adaptor molecule 1, amyloid precursor protein and receptor of advanced glycosylation end-products. After intervention with LBP, the above changes were significantly reduced. Remarkably, morphological remodeling of blood vessel-associated retinal astrocytes, marked by glial fibrillary acidic protein, was also observed. These results, taken together, suggest that LBP regulated the production of amyloid-β and expression of receptor of advanced glycosylation end-products, as well as mediating the activity of retinal glial cells, which may lead to the promotion of better maintenance of the blood-retinal barrier and improved neuronal survival in AOH insult. This study was approved by the Committee for the Use of Live Animals in Teaching and Research (approval No. CULTRA-#1664-08).

Key Words: *astrocyte; blood-retinal barrier; glial cell; Lycium barbarum; microglia; model; plasticity; remodel; retina*

Chinese Library Classification No. *R453; R774.6; R741*

Introduction

Neurodegeneration of retinal ganglion cells (RGCs) in glaucoma goes through two phases: 1) direct damage to cell bodies and their axons, and 2) secondary damage due to responses by non-neuronal cells. Among these, the secondary damage is considered to be the major cause of RGC loss (Tombran-Tink et al., 2008), with the reactivity of glial cells playing an important role. Previous studies showed that astrocytic gliosis in the optic nerve head was closely associated with the degeneration of optic nerve axons (Prasanna et al., 2011; Howell et al., 2014; Schneider and Fuchshofer, 2016). However, details of the reactivity of retinal glial cells in acute ocular hypertension (AOH) conditions during the development of RGC degeneration are still unclear.

AOH, including injury due to ischemia and mechanical high pressure, commonly exists in the progress of glaucomatous neuropathy. The advantage of an AOH animal model is that it can simulate the pathophysiological mechanism of an acute attack of glaucoma, to highlight the influence of ischemia-reperfusion and damage to the blood-retinal barrier in the pathogenesis of RGC degeneration. In addition, AOH is a convenient *in vivo* model for the study of neuroprotective mechanisms. Our previous studies verified that Lycium barbarum polysaccharides (LBP), a kind of traditional Chinese medicine extract, exhibits neuroprotective effects in ischemia/reperfusion models and glaucomatous animals (Chiu et al., 2010; Li et al., 2011; Mi et al., 2012b; Yang et al., 2017). Recently, it was reported that regardless of whether the administration was pretreatment or posttreatment, LBP could protect RGCs in AOH insult, with improvements in visual function in an animal-behavior test, electroretinography and the thickness of the optic nerve fiber layer (Lakshmanan et al., 2019a, b). Thus, the underling protective mechanisms of LBP in neurodegeneration need to be investigated.

As primary components in the neurovascular unit, glial cells play key roles in the pathogenesis of neurodegeneration in the retina and central nervous system (CNS) (Deane et al., 2003). Microglia activation is reportedly involved in the pathogenesis of RGC degeneration in different murine glaucoma models (Chiu et al., 2009; Huang et al., 2018). However, the effects of LBP on retinal glial reactivity are unclear.

The toxic impact of amyloid-β (Aβ) on neurons is seen in many CNS diseases, such as Alzheimer's disease (Ning et al., 2008). As the receptor for advanced glycation endproducts (AGEs), receptor of advanced glycosylation end-products (RAGE) can bind multiple ligands, such as AGEs, and neuronal toxicants, such as Aβ, which cause neurodegeneration in CNS. Over-expression of RAGE on blood vessel endothelial cells can promote the transportation of circulating Aβ and AGEs, to accumulate into the parenchyma and cause the release of endothelin-1 (ET-1) (Deane et al., 2003). In our previous study, we verified the above-described role of vascular RAGE and observed over-expression of Aβ on retinal neurons in an AOH model (Mi et al., 2012a). However, it is not known whether vascular RAGE is the only pathway for the production of Aβ. Therefore, we have evaluated the effect of LBP on the reactivity of retinal glial cells and investigated the relationship between retinal gliosis and Aβ toxicity in AOH.

Materials and Methods

Animals

Male C57BL/6N mice (aged 10–12 weeks, weight 20–25 g) were used in this study, in order to be consistent with our previous research into LBP (Mi et al., 2012a). The animal feeding environment was maintained on a 12-hour light–dark cycle and the mice received food and water *ad libitum*. All animals were specific-pathogen-free level, purchased from the University of Hong Kong, China. All experimental designs and protocols were approved by the Committee for the Use of Live Animals in Teaching and Research (approval No. CULTRA-#1664-08) on January 1, 2008, and conducted under the institutional guidelines for the care and use of laboratory animals at The University of Hong Kong, China.

Establishing the mouse model of AOH

General anesthesia was administered to the animals through intraperitoneal injection of a mixture of ketamine (80 mg/kg) and xylazine (8 mg/kg). Topical eye drops were used for desensitizing the cornea, with proparacaine hydrochloride 0.5% (Alcaine; Alcon, Ltd., Fort Worth, TX, USA), and dilating the pupil (Mydriacyl, Alcon, Ltd.). AOH was induced according to the procedure used in our previous study (Mi et al., 2012a). Briefly, a micro glass tube, linked to a reservoir of balanced salt solution (Alcon, Ltd.), was inserted into the anterior chamber of one eye/animal for 60 minutes, to increase the intraocular pressure to 90 mmHg and maintain it at that level. To keep the animal's temperature at 37 ± 0.5°C, a heating pad was used during the surgical procedure. Tobramycin ointment (0.3%; Alcon, Ltd.) was applied to the conjunctival sac to prevent infection after the AOH operation.

Drug administration

Based on the finding in our previous study that pretreatment with LBP from 7 days before AOH could effectively rescue RGCs, we used the same protocol for LBP administration (Mi et al., 2012a). LBP was extracted from dried fruits of Lycium barbarum (Ningxia, China) by decoloration and delipidation in alcohol, and boiling in distilled water by Shanghai Institute of Materia Medica, Chinese Academy of Sciences. The extract was then freeze-dried into powder for storage. For experimental use, the LBP solution was freshly prepared by dissolving the powder in phosphate-buffered saline (PBS; 0.01 M, pH 7.4) before use, as previously reported in our lab (Mi et al., 2012b; Yang et al., 2017). The mice were randomly assigned to two treatment groups (n = 7 per group), one for oral feeding with LBP (1 mg/kg) and the other, with PBS vehicle. Daily gavage was performed with a feeding needle, from 7 days before AOH until sacrifice for sampling.

Sample processing

On the fourth day after the AOH operation, the mice were sacrificed, using an overdose of sodium pentobarbital. The eyeballs were removed while fresh and fixed in 4% para-

formaldehyde at 4°C overnight (retinal flat-mounts for 2–4 hours). Samples were dehydrated with a graded series of ethanol and xylene, and subsequently embedded in paraffin wax with a clear orientation marking the 12 o'clock position on each eyeball. Seven-μm-thick cross-sections were cut.

Immunohistochemistry analysis

Retinal samples were rinsed with PBS, and kept in a solution of PBS with 0.3% Triton X-100 (Sigma, Darmstadt, Germany) and 10% goat serum (Sigma) for 1 hour. Then, they were incubated with different primary antibodies (**Table 1**) overnight at 4°C, followed by incubation with a second set of antibodies. Cross-sections were incubated with fluorescent secondary antibodies (**Table 1**) for 2 hours at room temperature, or with biotinylated secondary antibodies for 1 hour, followed by conjugation with an avidin-biotin-peroxidase-complex kit and detection of diaminobenzidine. Flat-mounted retinas were incubated with the secondary antibody at 4°C overnight. A diamidino-2-phenylindole (0.2%) staining procedure was used in some conditions to visualize the nucleus. After these procedures, the retinal sections or flat-mounts were observed under a fluorescent microscope (Zeiss, Oberkochen, Germany) or confocal laser scanning microscope (LSM 510 Meta, Zeiss).

Histological evaluations

Astrocytes were labeled with S-100 on flat-mounted retinas and counted under an eye-piece grid of 200 × 200 μm^2 along the median line of each quadrant, starting from the optic disc to the border, at 400-μm intervals. Six microscopic fields for each quadrant, for a total of 24 per retina, were counted. This method was described previously (Fu et al., 2008).

For quantification of ionized calcium-binding adaptor molecule 1 (Iba-1)(+) microglia and neuronal RAGE expressed on RGCs, at least ten discontinuous sections from each animal were randomly chosen. We have previously reported this method (Mi et al., 2012a). On retinal cross-sections, Iba-1(+) microglia were counted only if the cell body was stained. Signals from processes without a labeled soma were not counted. For consistency, the sections containing the optic nerve stump were used, and at least three discontinuous sections (per animal) were analyzed. Images at 400× magnification of the middle retina at 1.1 mm on both sides of the optic nerve head (Chi et al., 2010) were analyzed using Stereo Investigator® software (MBF Bioscience-Micro-BrightField, Inc., Williston, Vermont, USA). RAGE staining intensity in neurons was analyzed using immunohistochemistry scores, as described in a previous study (Li et al., 2011). Briefly, three photographs at 400× magnification were taken on each side of the retina, from the central, middle and peripheral areas. The immunohistochemistry scores were evaluated according to the immunostaining intensity and the numbers of cells with positive signals. Then the average staining intensity (per cell) of neuronal RAGE was given by scoring RAGE-labeled neurons in the ganglion cell layer (GCL) versus the number of diamidino-2-phenylindole-labeled neurons in the GCL.

Statistical analysis

The non-AOH control group was composed of the contralateral eyes of mice from the PBS-fed-AOH group and the LBP-fed-AOH group. The data from the PBS-fed-AOH group were compared with the non-AOH control group to evaluate the AOH injury. The data from the LBP-fed-AOH group were compared with the PBS-fed-AOH group and non-AOH control group to evaluate the effects of LBP on AOH injury. Data analyses were performed in a blinded manner, to eliminate subjective bias. The slides were analyzed by observers blinded to the group of each mouse. Data were assembled as the mean ± standard deviation (SD) and then analyzed by one-way analysis of variance using GraphPad Prism software 7.0 (GraphPad Software Inc., San Diego, CA, USA). The statistically significant difference was set at $P < 0.05$.

Results

LBP reduces retinal gliosis in the AOH retina

Immunoreactivity of GFAP

Increased expression of glial fibrillary acidic protein (GFAP)

Table 1 Antibodies for the immunohistochemistry study

Antibody	Dilution	Host	Source	Catalog No.
S-100	1:200	Rabbit	Abcam, Cambridge, MA, USA	ab868
Glutamine synthetase	1:600	Mouse	Millipore, Burlington, MA, USA	MAB302
Glial fibrillary acidic protein	1:400	Mouse	Sigma, Darmstadt, Germany	G3893
Glial fibrillary acidic protein	1:1000	Rabbit	Dako, Kyoto, Japan	Z0334
Aquaporin-4	1:400	Rabbit	Millipore, Burlington, MA, USA	AB3594
Ionized calcium binding adaptor molecule 1	1:800	Rabbit	Wako, Osaka, Japan	019-19741
Receptor of advanced glycosylation end-products	1:200	Rabbit	Abcam, Cambridge, UK	ab3611
Amyloid precursor protein	1:100	Mouse	Millipore, Burlington, MA, USA	MAB348
Alexa Fluor 568 (goat anti-rabbit)	1:200		Molecular Probes, Waltham, MA, USA	A11036
Alexa Fluor 488 (goat anti-mouse)	1:200		Molecular Probes, Waltham, MA, USA	A11029
Alexa Fluor 350 (goat anti-rabbit)	1:200		Molecular Probes, Waltham, MA, USA	A21068
Diamidino-2-phenylindole	1:5000		Sigma, Darmstadt, Germany	D9564
Biotinylated goat anti-rabbit immunoglobulin	1:200		Dako, Kyoto, Japan	E0432
Diaminobenzidine kit			Invitrogen, Waltham, MA, USA	2114

in retinal astrocytes and Müller cells has been interpreted as a gliosis marker under stress conditions, as has been reported in many studies involving the retina and brain (Wang et al., 2018; Rattner et al., 2019), and it was also true in the AOH retina (Hirrlinger et al., 2010). In the present study, we verified Hirrlinger et al.'s (2010) result. In the non-AOH control retina, positive GFAP staining was found in astrocytes in the GCL and around retinal blood vessels in the inner nuclear layer (**Figure 1A**). Contrary to that, there was an obvious increase in GFAP staining in the processes of Müller cells and in the astrocytes around retinal blood vessels in the PBS-fed-AOH group (**Figure 1B**). However, in the LBP-fed-AOH group (**Figure 1C**) the processes of the Müller cells were not stained.

Effects of LBP on the numbers of retinal astrocytes

To further evaluate the effect of LBP on retinal gliosis, S-100 was used to detect the cell bodies of retinal astrocytes and to count the cell numbers on retinal flat-mounts. Compared with the non-AOH control (**Figure 2A**), the number of S-100-labeled astrocytes was increased in the PBS-fed-AOH group (**Figure 2B**). However, in the LBP-fed-AOH group, it was lower than in the PBS-fed-AOH group and similar to the number in the non-AOH control retina (**Figure 2C**). The cell counts demonstrated that retinal gliosis was significantly decreased in the LBP-fed-AOH group *versus* the PBS-fed-AOH ($P < 0.05$), although there was still evidence of gliosis in the LBP-fed-AOH group when compared with the non-AOH control ($P < 0.05$; **Figure 2D** and **E**).

Effects of LBP on morphological remodeling of blood vessel-associated astrocytes

GFAP staining was also used on retinal flat-mounts to observe the morphological changes of the retinal astrocytes located around blood vessels. Compared with the non-AOH control retina (**Figure 3A**), in the PBS-fed-AOH group (**Figure 3B**), the GFAP-stained astrocytes appeared as masses of cell bodies and processed similar to uncombed hair; however, in the LBP-fed-AOH group (**Figure 3C**), the processes of astrocytes were arranged more smoothly than in the PBS-fed-AOH group. In addition, there appeared to be more processes of astrocytes contacting the blood vessels when compared with the non-AOH control, suggesting a new and different pattern of endfeet contact around blood vessels. We also checked the contralateral eyes of animals in the group with LBP treatment and AOH insult, but did not observe similar morphological changes of the endfeet of retinal astrocytes when compared with the injured eye (data not shown here).The key enzyme in glutamate-glutamine cycling, glutamine synthetase (GS), was used to detect functional changes in glutamine metabolism in astrocytes (**Figures 3D–F**). In the non-AOH control retina (**Figure 3G**), there was no co-labeling signal, suggesting that GS is not expressed on astrocytes in the normal retina, which agrees with previous reports (Zhang et al., 2009; Coucha et al., 2019; Mages et al., 2019). However, in the PBS-fed-AOH group, most astrocytes showed yellow, co-labeled GS signals (**Figure 3H**). In a previous study, it was suggested that the expression level of GS in Müller cells did not change in AOH (Hirrlinger et al., 2010). Here, using the method of co-labeled staining on flat-mounted retinae, our data clearly showed up-regulation of expression of GS in astrocytes, suggesting that increased glutamate toxicity was present in astrocytes after AOH stress. In the LBP-fed-AOH group (**Figure 3I**), the labeling color in most astrocytes was green, suggesting that there was a decrease in glutamine toxicity in retinal astrocytes when treated with LBP.

Immunoreactivity of aquaporin-4

Aquaporin-4 (AQP-4) is a marker reflecting the capability of the balancing water across the wall of blood vessels, which can also be used to detect functional changes in glial cells and astrocytes (Catalin et al., 2018). In normal con-ditions, seen in the non-AOH control retinae (**Figure 4A** and **D**), light AQP-4 staining signals were seen in the pro-cesses of Müller cells, in the inner plexiform layer and in their endfeet in the internal and external limiting membranes, and in the retinal blood vessels. In the PBS-fed-AOH group (**Figure 4B** and **E**), strong staining was observed not only in the processes and endfeet of Müller cells, but also in their cell bodies associated with the strong signals around blood vessels, suggesting that the strong signaling of AQP4 around blood vessels is a response of the endfeet of astrocytes. However, in the LBP-fed-AOH group (**Figure 4C** and **F**), the staining was comparable to the level in the non-AOH control group. Using co-labeling staining of AQP-4 with GFAP in retinal flat-mounts, the astrocytes showed extraordinary morphological changes in the PBS-fed-AOH group at some locations around the blood vessels, associated with the extensive expression of AQP-4 (**Figure 4E** and **H**). However, in the LBP-fed-AOH group (**Figure 4F** and **I**), with lower expression of AQP-4 around blood vessels, the endfeet of astrocytes also showed different shapes when compared with the non-AOH controls (**Figure 4D** and **G**). Thus, these data suggest that AOH induced degenerative changes to retinal astrocytes, associated with possible loss of the function of their endfeet around blood vessels, whereas LBP treatment made the endfeet of astrocytes more resistant to the insult of AOH.

Reactivity of retinal microglia/macrophages

The effect of LBP to reduce gliosis was also observed in other cell types, such as the microglia and macrophages. Compared with the non-AOH control retina (**Figure 5A**), in the PBS-fed-AOH group, there was a clear increase in the number of Iba-1-labeled microglia and macrophages in retinal tissue (**Figure 5B**). However, in the LBP-fed-AOH group, this number was lower (**Figure 5C**) than in the PBS-fed-AOH group, but still higher than in the non-AOH control group (**Figure 5A**). Quantification of these numbers showed significant differences between the three groups ($P < 0.05$; **Figure 5D**).

LBP down-regulates the expression of APP

Amyloid precursor protein (APP) is the key material for

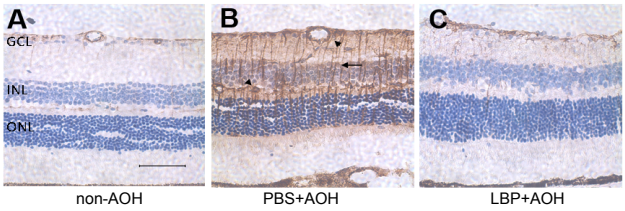

Figure 1 Expression of GFAP is down-regulated in LBP-fed-AOH retinae at 4 days after AOH.
(A–C) Representative photographs of GFAP-stained retinal sections in the non-AOH control group (non-AOH; A), PBS-fed-AOH group (PBS + AOH; B) and LBP-fed-AOH group (LBP + AOH; C). Note the strong GFAP staining in the processes of Müller cells (arrow) and the astrocytes (arrowheads) around retinal blood vessels in (B), compared with the staining in (C) and (A). Scale bar: 50 μm. AOH: Acute ocular hypertension; GCL: ganglion cell layer; GFAP: glial fibrillary acidic protein; INL: inner nuclear layer; LBP: Lycium barbarum polysaccharides; ONL: outer nuclear layer; PBS: phosphate-buffered saline.

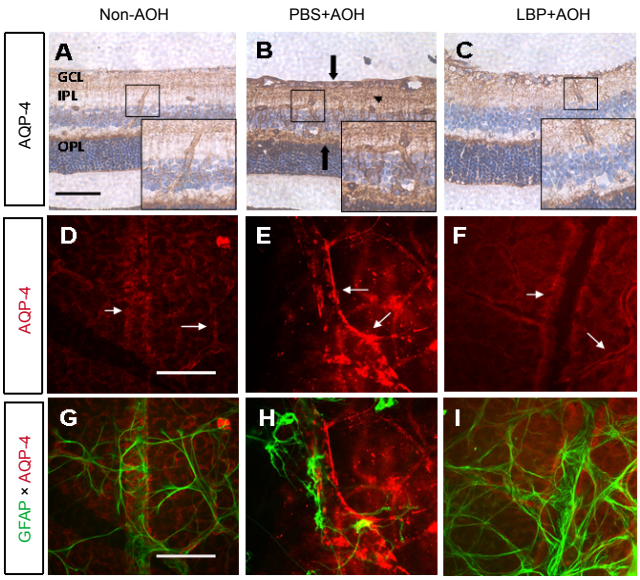

Figure 4 Alteration of AQP-4 and morphological remodeling of blood-vessel-associated astrocytes in LBP-fed-AOH retinae at 4 days after AOH.
(A–C) Representative photos of AQP-4 immunostaining on retinal sections in the non-AOH control (non-AOH; A), PBS-fed-AOH (PBS + AOH; B) and LBP-fed-AOH (LBP + AOH; C) groups. Note that the enlarged boxes in A–C show that the signals of AQP-4 on the blood vessels and the cell bodies of Müller cells were stronger in B than in A and C. The arrowhead in B indicates the strong signal of AQP-4 in the processes of Müller cells in the IPL; and the arrows in B show the strong signal of AQP-4 in the endfeet of Müller cells in the internal limiting membrane and external limiting membrane. (D–F) Representative photographs of AQP-4 immunostaining on retinal flat-mounts, in the non-AOH control group (D), PBS-fed-AOH group (E) and LBP-fed-AOH group (F). Note the signals of AQP-4 around retinal blood vessels (white arrows). (G–I) Merged photographs of GFAP (green, marked by Alexa Fluor 488) and AQP-4 (red, marked by Alexa Fluor 568) on retinal flat-mounts, in the non-AOH control group (G), PBS-fed-AOH group (H) and LBP-fed-AOH group (I). Scale bars: 50 μm. AOH: Acute ocular hypertension; AQP-4: aquaporin-4; GCL: ganglion cell layer; GFAP: glial fibrillary acidic protein; IPL: inner plexiform layer; LBP: Lycium barbarum polysaccharides; OPL: outer plexiform layer; PBS: phosphate-buffered saline.

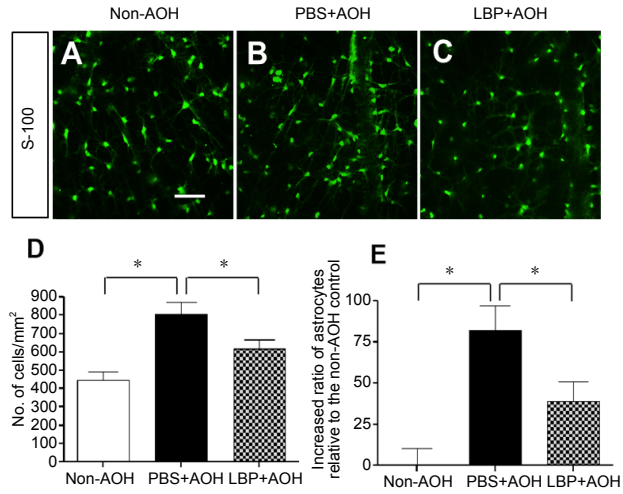

Figure 2 Decrease in the number of S-100-labeled astrocytes in LBP-fed-AOH retinae at 4 days after AOH.
(A–C) Representative photographs of S-100-labeled astrocytes (green, marked by Alexa Fluor 350) on retinal flat-mounts, in the non-AOH control group (non-AOH; A), PBS-fed-AOH group (PBS + AOH; B) and LBP-fed-AOH group (LBP + AOH; C). Scale bar: 50 μm. (D) Quantification of the numbers of astrocytes in 1 mm^2. (E) Quantification of the increased ratio of astrocytes relative to the non-AOH control. Data are presented as the mean ± SD (n = 7 per group). $*P < 0.05$ (one-way analysis of variance). AOH: Acute ocular hypertension; LBP: Lycium barbarum polysaccharides; PBS: phosphate-buffered saline.

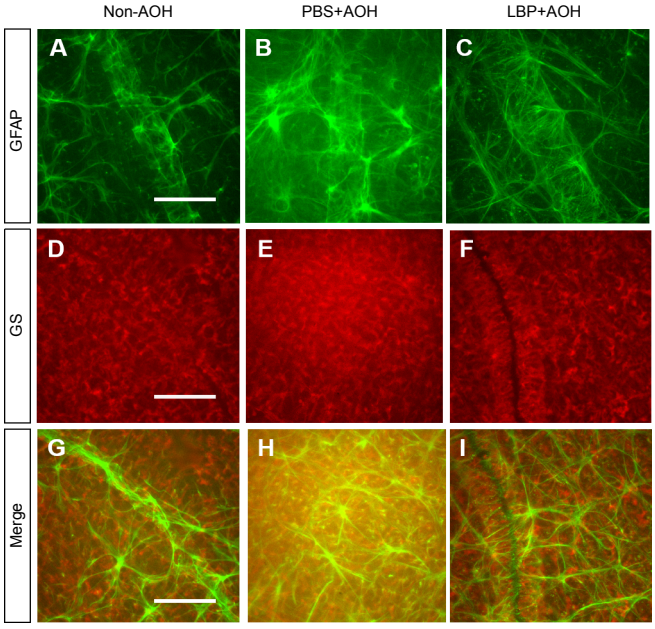

Figure 3 Morphological remodeling of blood vessel-associated astrocytes in LBP-fed-AOH retinae at 4 days after AOH.
(A–C) Representative photographs of GFAP-stained astrocytes on retinal flat-mounts, in the non-AOH control group (non-AOH; A), PBS-fed-AOH group (PBS + AOH; B) and LBP-fed-AOH group (LBP + AOH; C). (D–F) GS immunostaining of retinal flat-mounts in the non-AOH control group (D), PBS-fed-AOH group (E) and LBP-fed-AOH group (F). (G–I) Merged photographs of GFAP (green, marked by Alexa Fluor 488) and GS (red, marked by Alexa Fluor 568) on retinal flat-mounts in the non-AOH control group (G), PBS-fed-AOH group (H) and LBP-fed-AOH group (I). Scale bars: 50 μm. AOH: Acute ocular hypertension; GFAP: glial fibrillary acidic protein; GS: glutamine synthetase; LBP: Lycium barbarum polysaccharides; PBS: phosphate-buffered saline.

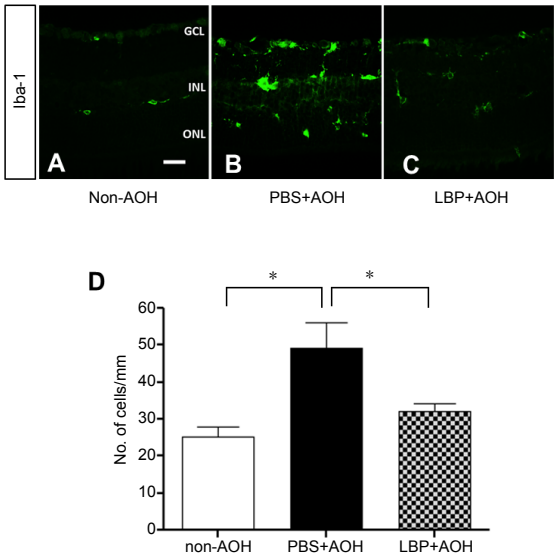

Figure 5 Decreased number of Iba-1(+) cells in LBP-fed-AOH retinae at 4 days after AOH.
(A–C) Representative photographs of Iba-1-stained microglia and macrophages (green, marked by Alexa Fluor 350) on retinal sections, in the non-AOH control group (non-AOH; A), PBS-fed-AOH group (PBS + AOH; B) and LBP-fed-AOH group (LBP + AOH; C). Scale bar: 50 μm (D) Quantification of cells. Data are presented as the mean ± SD (n = 7 per group). $*P < 0.05$ (one-way analysis of variance). AOH: Acute ocular hypertension; GCL: ganglion cell layer; Iba-1: ionized calcium-binding adaptor molecule 1; INL: inner nuclear layer; LBP: Lycium barbarum polysaccharides; ONL: outer nuclear layer; PBS: phosphate-buffered saline.

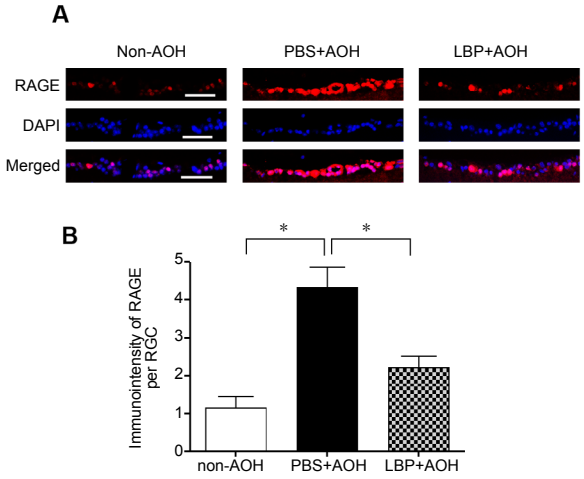

Figure 7 Up-regulation of the expression of RAGE in neurons of PBS-fed retinae and down-regulation in LBP-fed retinae at 4 days after AOH.
(A) Representative photographs of RAGE-stained neurons in the ganglion cell layer on retinal sections in the non-AOH control (non-AOH), PBS-fed-AOH (PBS + AOH) and LBP-fed-AOH (LBP + AOH) groups. Scale bars: 20 μm. (B) Quantification of the immunointensity of neuronal RAGE. Data are presented as the mean ± SD (n = 7 per group). $*P < 0.05$ (one-way analysis of variance). AOH: Acute ocular hypertension; DAPI: diamidino-2-phenylindole; LBP: Lycium barbarum polysaccharides; PBS: phosphate-buffered saline; RAGE: receptor of advanced glycosylation end-products; RGC: retinal ganglion cell.

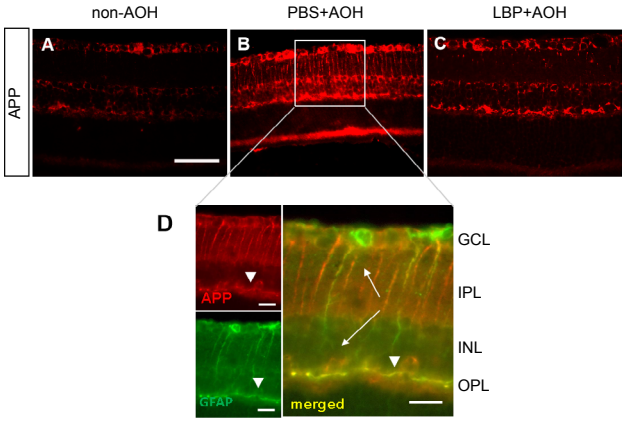

Figure 6 Up-regulation of the expression of APP in PBS-fed retinae and down-regulation in LBP-fed retinae at 4 days after AOH.
(A–C) Representative photographs of APP immunostaining on retinal sections in the non-AOH control group (non-AOH; A), PBS-fed-AOH group (PBS + AOH; B) and LBP-fed-AOH group (LBP + AOH; C). (D) Enlarged photographs from the PBS-fed-AOH retina show the co-localization of GFAP and APP, confirming the presence of APP staining in the processes of Müller cells in the IPL (arrows) and in astrocytes or the processes of Müller cells in the OPL (arrowheads). Scale bars: 50 μm in A–C; 20 μm in D. AOH: Acute ocular hypertension; APP: amyloid precursor protein; GCL: ganglion cell layer; GFAP: glial fibrillary acidic protein; INL: inner nuclear layer; IPL: inner plexiform layer; LBP: Lycium barbarum polysaccharides; OPL: outer plexiform layer; PBS: phosphate-buffered saline.

the production of $A\beta_{1-42}$. APP was detected in the retinae of chronic ocular hypertension rats (McKinnon et al., 2002). In the present study, mild positive APP staining in the outer plexiform layer and the neurons of the GCL was detected in the non-AOH control retinae (**Figure 6A**). In the PBS-fed-AOH group, strong APP staining was observed not only in the outer plexiform layer and neurons of the GCL, but also in the processes of Müller cells in the inner plexiform layer (**Figure 6B**). Co-labeling with GFAP showed that some of the positive APP signals found in the outer plexiform layer belonged to astrocytes or the processes of Müller cells around blood vessels. In addition, the processes in the inner plexiform layer were confirmed to belong to activated Müller cells (**Figure 6D**), which have previously been reported to express GFAP under stress conditions (Hirrlinger et al., 2010). In the LBP-fed-AOH group (**Figure 6C**), the expression of APP was lower than in the PBS group; however, some strong APP-stained signals were still found in the GCL and outer plexiform layer. This result could be attributed to astrocytic gliosis in the LBP-fed-AOH group.

LBP down-regulates the expression of RAGE on RGCs

The neurons in the GCL and inner nuclear layer showed similar levels of staining in the non-AOH and AOH conditions, and therefore we analyzed neurons in the GCL to examine the expression level of neuronal RAGE in the retina. Semi-quantification analysis showed that the relative staining intensity of neuronal RAGE in the PBS-fed-AOH group was higher than that in the non-AOH group ($P < 0.05$), but lower than that in the LBP-fed-AOH group ($P < 0.05$; **Figure 7A** and **B**). Although the number of surviving neurons was

lowest in the PBS-fed-AOH group, the semi-quantitative analysis suggested that the staining density of RAGE per neuron in the PBS-fed-AOH group was the highest, when compared with the other two groups; and feeding LBP to the mice decreased the expression of RAGE in the neurons.

Discussion

Along with the damage to retinal neurons and vasculature reported in our previous study (Mi et al., 2012a), in the present study, we demonstrated that transient elevation of intraocular pressure to 90 mmHg for 60 minutes induced extensive retinal gliosis. LBP treatment reduced the glial activation and decreased the RAGE-associated damage to retinal neurons. However, a limitation of this study is that the intraocular pressure induced in the experiment is much higher than that caused by the clinical disease. The main mechanism of AOH is ischemia/reperfusion injury, which only represents part of the pathogenesis of glaucoma and does not reflect the whole pathological process.

AOH insult induces damage to many components of the neurovascular unit in the retina. Besides degeneration of neurons, retinal gliosis is another negative consequence. In CNS degeneration, it has been reported that astrocyte gliosis could activate microglia cells associated with the release of inflammatory factors, oxidative stress and other damage to the tissue, which could threaten the survival of neurons (Duncombe et al., 2017; Magaki et al., 2018). Thus, reduction of gliosis has been considered a kind of neuroprotection. Our previous study showed the effect of LBP on the reduction of expression of GFAP after middle cerebral artery occlusion injury (Li et al., 2011). In the present study, we verified this effect of LBP in the AOH model, together with demonstrating a decreased number of astrocytes. The possible mechanism is related to the effect of LBP on regulation of ET-1 because ET-1 promotes astrocyte proliferation *in vitro* and *in vivo*, which was verified in the ocular hypertension rat model (Prasanna et al., 2011). Our previous study showed that there was an up-regulation of ET-1 in the AOH retina and that the up-regulation was reversed by LBP treatment (Mi et al., 2012a), suggesting that LBP could inhibit the proliferation of retinal astrocytes in AOH by regulating the expression of ET-1.

In addition to gliosis, we detected obvious morphological changes in the endfeet of astrocytes around blood vessels. This included enrichment of GFAP staining in their cell bodies and reduction of their endfeet touching blood vessels. Together with the up-regulated expression of GS in astrocytes and the increased expression of AQP-4 around the nearby wall of blood vessels, these changes in astrocytes may be a form of structural and functional degeneration. The increase in expression of GS and AQP-4 has been reported to cause damage to tissues in ischemia (Zhang et al., 2009; Li et al., 2011). Moreover, we found in the LBP-treated AOH retina that the blood vessel-associated astrocytes showed entirely different morphology compared with the PBS-fed AOH retina and even with the non-AOH retina. The remarkably remodeled astrocytes appeared to have smoothly arranged processes, and more processes touching the blood vessels, but lacking the edema-induced enlargement of their endfeet seen in similar ischemic conditions (Yeung et al., 2009; Li et al., 2011). Considering the protective effect of LBP on neurons and blood vessel cells seen in our previous study (Mi et al., 2012a), this kind of morphological remodeling of astrocytes might be beneficial to the integrity of the blood-retinal barrier and to resisting ischemic insults. Together with our previous data showing that LBP protected vascular cells and decreased IgG leakage (Mi et al., 2012a), we can conclude that LBP promotes maintenance of the blood-retinal barrier through several pathways.

Microglia, another type of retinal glial cells, play a key role in immune mediation under ischemic damage (Rayasam et al., 2018). Iba-1 is a general marker, which can label all of the retinal microglia/microphage in both the resting and activated states. Previous studies verified that in AOH insult there was an increased number of activated retinal microglia with phagocytic properties, which played a pathogenic role in RGC death. Thus, decreasing the number of microglia is neuroprotective for RGC survival (Wang et al., 2014; Huang et al., 2018). In the optic nerve transection RGC-injury model, it was reported that LBP affected retinal microglial polarization, with decreased MI and increased M2, together with decreasing the production of pro-inflammatory cytokines and increasing the production of anti-inflammatory cytokines (Li et al., 2019). Thus, the inhibitory effect of LBP on the increase in the number of microglia observed in this study is neuroprotective.

In the neurovascular unit, cell-cell crosstalk between astrocytes and microglia has been confirmed recently (Pierozan et al., 2016; MacLean et al., 2019; Subauste, 2019). In this study, our data showed that LBP decreased the activation of microglia and astrocytes, suggesting that reduced activity of microglia might also be a kind of cooperative mechanism, contributing to the functional recovery of the microenvironment and neurovascular unit under AOH conditions. A similar effect of LBP was reported in our previous study using a chronic glaucoma model, which suggested that LBP has protective effects on the survival of RGCs (Chiu et al., 2009; Huang et al., 2018). In CNS injury, a high level of S-100 production in astrocytes may contribute to inducible nitric oxide synthase and nitric oxide production in microglia, causing activated astrocytes to participate in immune regulation of microglia (Donato et al., 2009). As a marker of astrogliosis, expression of S-100 was down-regulated by LBP treatment in this study, indicating that the activation of microglia was also down-regulated by LBP through cell-cell crosstalk. Regarding the repair process in the LBP-fed AOH retina, how to regulate the beneficial crosstalk between astrocytes and microglia should be further investigated.

RAGE could mediate multiple signaling pathways to promote Aβ-induced neurodegeneration. Vascular RAGE could serve as a cross-membrane transporter for the deposition of Aβ in tissue (Criscuolo et al., 2017; Lana et al., 2017; MacLean et al., 2019). Our previous study revealed elevated RAGE expression in many cell types in the AOH retina (Mi et

al., 2012a). In this study, we detected elevated RAGE expression on RGCs, suggesting that neuronal RAGE may contribute to Aβ production on neurons directly, without cell-cell signaling transportation. In addition, we observed up-regulation of APP in RGCs, suggesting the involvement of APP in the production of Aβ in AOH conditions. As an essential precursor of Aβ, increased APP has been verified to promote the production of Aβ by upregulating b-secretase expression and activity in ischemia (Zhiyou et al., 2009; Xie et al., 2017). Thus, it is possible that RAGE regulates β-site APP-cleaving enzyme 1, to generate Aβ from APP (Cho et al., 2009). In the AOH retinae in this study, we also found up-regulation of APP in astrocytes and Müller cells. Together with the elevation of glial RAGE observed in our previous AOH study (Mi et al., 2012a), retinal gliosis in AOH affects multiple signaling pathways in the neurovascular unit. However, the related molecular mechanisms need to be further investigated.

Our previous study reported that in AOH insult, there was an increased expression of Aβ on RGCs. Treatment with LBP could reduce the transportation of circulating Aβ by regulating the expression of vascular RAGE (Mi et al., 2012a). In this study, we showed that LBP reduced the expression of neuronal RAGE on RGCs, suggesting that regulation of the APP-RAGE axis may be another way for LBP to reduce the production of Aβ in neurons. It is known that Aβ is neurotoxic. Our previous studies demonstrated that LBP could protect cerebral neurons from Aβ toxicity *in vitro* and *in vivo* (Yu et al., 2007; Ho et al., 2009). Thus, in the AOH condition, as in many ischemic retinopathies, LBP could regulate the expression of RAGE in different cell types to decrease Aβ levels in the retina, to recover the stability of the microenvironment.

In this study, we gave the animals LBP as a pretreatment, before initiating AOH. According to previous studies, the pretreatment approach to LBP administration has been found to have neuroprotective effects in different animal models of retinal neuronal degeneration (Chiu et al., 2009; Mi et al., 2012a; Yang et al., 2017). In a recent study, post-treatment with LBP was also reported to protect RGCs in an AOH model (Lakshmanan et al., 2019a). In a clinical trial with patients who had retinitis pigmentosa, daily consumption of Lycium barbarum granules showed neuroprotective effects, to improve the outcome for the patients in terms of visual acuity, visual fields and electroretinograms (Chan et al., 2019). In that trial, the daily supplement of Lycium barbarum granules contained 175 mg of LBP, which is higher than the dosage used in our study. There are many differences between human and the animal models, but it is suggested that a daily supplement of LBP may be neuroprotective for ocular hypertensive patients.

In summary, our results revealed that the neuroprotective action of LBP is related to regulating the reactivity of retinal glial cells. The remodeling effect of astrocytes around blood vessels may be a target of LBP for blood vessel protection. The anti-RAGE effect of LBP could be a novel way by which the retina is protected after damage or disease.

Author contributions: *Study conception and designer: KFS, SKC, ACYL, RCCC; data collection and integration: XM, QF; data analysis: XSM, QF; manuscript writing: XSM; manuscript review: KFS, SKC, ACYL, RCCC; statistical processor: XM, QF; fund director: KS. The provider of technology: XSM, QF. The research director: KFS. All authors approved the final version of the manuscript.*
Conflicts of interest: *There were no conflicts of interest in this experiment.*
Financial support: *This study was supported in part by the National Basic Research Program of China, No. 81300766 (to XSM); the Cultivation and Innovation Fund from the First Affiliated Hospital of Jinan University, China, No. 802168 (to XSM); Hygiene & Health Appropriated Technology and Promoting Project of Guangdong Province of China, No. 201905270933056876 (to XSM); the fund of Leading Talents of Guangdong Province of China, No. 87014002 (to KFS); a grant from Ningxia Key Research and Development Program, and Programme of Introducing Talents of Discipline to Universities of China, No. B14036 (to KFS). The funding sources had no role in study conception and design, data analysis or interpretation, paper writing or deciding to submit this paper for publication.*
Institutional review board statement: *This study was approved by the Committee for the Use of Live Animals in Teaching and Research (approval No. CULTRA-#1664-08) on January 1, 2008.*
Copyright license agreement: *The Copyright License Agreement has been signed by all authors before publication.*
Data sharing statement: *Datasets analyzed during the current study are available from the corresponding author on reasonable request.*
Plagiarism check: *Checked twice by iThenticate.*
Peer review: *Externally peer reviewed.*

References

Catalin B, Rogoveanu OC, Pirici I, Balseanu TA, Stan A, Tudorica V, Balea M, Mindrila I, Albu CV, Mohamed G, Pirici D, Muresanu DF (2018) Cerebrolysin and aquaporin 4 inhibition improve pathological and motor recovery after ischemic stroke. CNS Neurol Disord Drug Targets 17:299-308.

Chan HH, Lam HI, Choi KY, Li SZ, Lakshmanan Y, Yu WY, Chang RC, Lai JS, So KF (2019) Delay of cone degeneration in retinitis pigmentosa using a 12-month treatment with Lycium barbarum supplement. J Ethnopharmacol 236:336-344.

Chi ZL, Akahori M, Obazawa M, Minami M, Noda T, Nakaya N, Tomarev S, Kawase K, Yamamoto T, Noda S, Sasaoka M, Shimazaki A, Takada Y, Iwata T (2010) Overexpression of optineurin E50K disrupts Rab8 interaction and leads to a progressive retinal degeneration in mice. Hum Mol Genet 19:2606-2615.

Chiu K, Chan HC, Yeung SC, Yuen WH, Zee SY, Chang RC, So KF (2009) Modulation of microglia by Wolfberry on the survival of retinal ganglion cells in a rat ocular hypertension model. J Ocul Biol Dis Infor 2:47-56.

Chiu K, Zhou Y, Yeung SC, Lok CK, Chan OO, Chang RC, So KF, Chiu JF (2010) Up-regulation of crystallins is involved in the neuroprotective effect of wolfberry on survival of retinal ganglion cells in rat ocular hypertension model. J Cell Biochem 110:311-320.

Cho HJ, Son SM, Jin SM, Hong HS, Shin DH, Kim SJ, Huh K, Mook-Jung I (2009) RAGE regulates BACE1 and Abeta generation via NFAT1 activation in Alzheimer's disease animal model. FASEB J 23:2639-2649.

Coucha M, Shanab AY, Sayed M, Vazdarjanova A, El-Remessy AB (2019) Modulating expression of thioredoxin interacting protein (TXNIP) prevents secondary damage and preserves visual function in a mouse model of ischemia/reperfusion. Int J Mol Sci 20:3969.

Criscuolo C, Fontebasso V, Middei S, Stazi M, Ammassari-Teule M, Yan SS, Origlia N (2017) Entorhinal cortex dysfunction can be rescued by inhibition of microglial RAGE in an Alzheimer's disease mouse model. Sci Rep 7:42370.

Deane R, Du Yan S, Submamaryan RK, LaRue B, Jovanovic S, Hogg E, Welch D, Manness L, Lin C, Yu J, Zhu H, Ghiso J, Frangione B, Stern A, Schmidt AM, Armstrong DL, Arnold B, Liliensiek B, Nawroth P, Hofman F, et al. (2003) RAGE mediates amyloid-beta peptide transport across the blood-brain barrier and accumulation in brain. Nat Med 9:907-913.

Donato R, Sorci G, Riuzzi F, Arcuri C, Bianchi R, Brozzi F, Tubaro C, Giambanco I (2009) S100B's double life: intracellular regulator and extracellular signal. Biochim Biophys Acta 1793:1008-1022.

Duncombe J, Lennen RJ, Jansen MA, Marshall I, Wardlaw JM, Horsburgh K (2017) Ageing causes prominent neurovascular dysfunction associated with loss of astrocytic contacts and gliosis. Neuropathol Appl Neurobiol 43:477-491.

Fu QL, Hu B, Wu W, Pepinsky RB, Mi S, So KF (2008) Blocking LINGO-1 function promotes retinal ganglion cell survival following ocular hypertension and optic nerve transection. Invest Ophthalmol Vis Sci 49:975-985.

Hirrlinger PG, Ulbricht E, Iandiev I, Reichenbach A, Pannicke T (2010) Alterations in protein expression and membrane properties during Müller cell gliosis in a murine model of transient retinal ischemia. Neurosci Lett 472:73-78.

Ho YS, Yu MS, Yik SY, So KF, Yuen WH, Chang RC (2009) Polysaccharides from wolfberry antagonizes glutamate excitotoxicity in rat cortical neurons. Cell Mol Neurobiol 29:1233-1244.

Howell GR, MacNicoll KH, Braine CE, Soto I, Macalinao DG, Sousa GL, John SW (2014) Combinatorial targeting of early pathways profoundly inhibits neurodegeneration in a mouse model of glaucoma. Neurobiol Dis 71:44-52.

Huang R, Liang S, Fang L, Wu M, Cheng H, Mi X, Ding Y (2018) Low-dose minocycline mediated neuroprotection on retinal ischemia-reperfusion injury of mice. Mol Vis 24:367-378.

Lakshmanan Y, Wong FSY, Zuo B, So KF, Bui BV, Chan HH (2019a) Posttreatment intervention with lycium barbarum polysaccharides is neuroprotective in a rat model of chronic ocular hypertension. Invest Ophthalmol Vis Sci 60:4606-4618.

Lakshmanan Y, Wong FS, Yu WY, Li SZ, Choi KY, So KF, Chan HH (2019b) Lycium barbarum polysaccharides rescue neurodegeneration in an acute ocular hypertension rat model under pre- and post-treatment conditions. Invest Ophthalmol Vis Sci 60:2023-2033.

Lana E, Khanbolouki M, Degavre C, Samuelsson EB, Åkesson E, Winblad B, Alici E, Lithner CU, Behbahani H (2017) Perforin Promotes Amyloid Beta Internalisation in Neurons. Mol Neurobiol 54:874-887.

Li HY, Huang M, Luo QY, Hong X, Ramakrishna S, So KF (2019) Lycium barbarum (Wolfberry) Increases retinal ganglion cell survival and affects both microglia/macrophage polarization and autophagy after rat partial optic nerve transection. Cell Transplant 28:607-618.

Li SY, Yang D, Yeung CM, Yu WY, Chang RC, So KF, Wong D, Lo AC (2011) Lycium barbarum polysaccharides reduce neuronal damage, blood-retinal barrier disruption and oxidative stress in retinal ischemia/reperfusion injury. PLoS One 6:e16380.

MacLean M, Derk J, Ruiz HH, Juranek JK, Ramasamy R, Schmidt AM (2019) The receptor for advanced glycation end products (RAGE) and DIAPH1: Implications for vascular and neuroinflammatory dysfunction in disorders of the central nervous system. Neurochem Int 126:154-164.

Magaki SD, Williams CK, Vinters HV (2018) Glial function (and dysfunction) in the normal & ischemic brain. Neuropharmacology 134:218-225.

Mages K, Grassmann F, Jägle H, Rupprecht R, Weber BHF, Hauck SM, Grosche A (2019) The agonistic TSPO ligand XBD173 attenuates the glial response thereby protecting inner retinal neurons in a murine model of retinal ischemia. J Neuroinflammation 16:43.

McKinnon SJ, Lehman DM, Kerrigan-Baumrind LA, Merges CA, Pease ME, Kerrigan DF, Ransom NL, Tahzib NG, Reitsamer HA, Levkovitch-Verbin H, Quigley HA, Zack DJ (2002) Caspase activation and amyloid precursor protein cleavage in rat ocular hypertension. Invest Ophthalmol Vis Sci 43:1077-1087.

Mi XS, Feng Q, Lo AC, Chang RC, Lin B, Chung SK, So KF (2012a) Protection of retinal ganglion cells and retinal vasculature by Lycium barbarum polysaccharides in a mouse model of acute ocular hypertension. PLoS One 7:e45469.

Mi XS, Chiu K, Van G, Leung JW, Lo AC, Chung SK, Chang RC, So KF (2012b) Effect of Lycium barbarum Polysaccharides on the expression of endothelin-1 and its receptors in an ocular hypertension model of rat glaucoma. Neural Regen Res 7:645-651.

Ning A, Cui J, To E, Ashe KH, Matsubara J (2008) Amyloid-beta deposits lead to retinal degeneration in a mouse model of Alzheimer disease. Invest Ophthalmol Vis Sci 49:5136-5143.

Pierozan P, Biasibetti H, Schmitz F, Ávila H, Parisi MM, Barbe-Tuana F, Wyse AT, Pessoa-Pureur R (2016) Quinolinic acid neurotoxicity: Differential roles of astrocytes and microglia via FGF-2-mediated signaling in redox-linked cytoskeletal changes. Biochim Biophys Acta 1863:3001-3014.

Prasanna G, Krishnamoorthy R, Yorio T (2011) Endothelin, astrocytes and glaucoma. Exp Eye Res 93:170-177.

Rattner A, Williams J, Nathans J (2019) Roles of HIFs and VEGF in angiogenesis in the retina and brain. J Clin Invest 130:3807-3820.

Rayasam A, Hsu M, Kijak JA, Kissel L, Hernandez G, Sandor M, Fabry Z (2018) Immune responses in stroke: how the immune system contributes to damage and healing after stroke and how this knowledge could be translated to better cures? Immunology 154:363-376.

Schneider M, Fuchshofer R (2016) The role of astrocytes in optic nerve head fibrosis in glaucoma. Exp Eye Res 142:49-55.

Subauste CS (2019) The CD40-ATP-P2X 7 receptor pathway: cell to cell cross-talk to promote inflammation and programmed cell death of endothelial cells. Front Immunol 10:2958.

Tombran-Tink J, Barnstable CJ, Shields MB (2008) Mechanisms of the glaucomas: disease processes and therapeutic modalities. Totowa, NJ, USA: Humana Press.

Wang K, Peng B, Lin B (2014) Fractalkine receptor regulates microglial neurotoxicity in an experimental mouse glaucoma model. Glia 62:1943-1954.

Wang X, Shu Q, Ni Y, Xu G (2018) CRISPR-mediated SOX9 knockout inhibits GFAP expression in retinal glial (Müller) cells. Neuroreport 29:1504-1508.

Xie H, Zhao Y, Zhou Y, Liu L, Liu Y, Wang D, Zhang S, Yang M (2017) MiR-9 regulates the expression of BACE1 in dementia induced by chronic brain hypoperfusion in rats. Cell Physiol Biochem 42:1213-1226.

Yang D, So KF, Lo AC (2017) Lycium barbarum polysaccharide extracts preserve retinal function and attenuate inner retinal neuronal damage in a mouse model of transient retinal ischaemia. Clin Exp Ophthalmol 45:717-729.

Yeung PK, Lo AC, Leung JW, Chung SS, Chung SK (2009) Targeted overexpression of endothelin-1 in astrocytes leads to more severe cytotoxic brain edema and higher mortality. J Cereb Blood Flow Metab 29:1891-1902.

Yu MS, Lai CS, Ho YS, Zee SY, So KF, Yuen WH, Chang RC (2007) Characterization of the effects of anti-aging medicine Fructus lycii on beta-amyloid peptide neurotoxicity. Int J Mol Med 20:261-268.

Zhang S, Wang H, Lu Q, Qing G, Wang N, Wang Y, Li S, Yang D, Yan F (2009) Detection of early neuron degeneration and accompanying glial responses in the visual pathway in a rat model of acute intraocular hypertension. Brain Res 1303:131-143.

Zhiyou C, Yong Y, Shanquan S, Jun Z, Liangguo H, Ling Y, Jieying L (2009) Upregulation of BACE1 and beta-amyloid protein mediated by chronic cerebral hypoperfusion contributes to cognitive impairment and pathogenesis of Alzheimer's disease. Neurochem Res 34:1226-1235.

C-Editor: Zhao M; S-Editors: Yu J, Li CH; L-Editors: Barnes C, Yu J, Song CP; T-Editor: Jia Y